Towards Near-Field 3D Spot Beamfocusing: Possibilities, Challenges, and Use-cases

Mehdi Monemi, *Member*, IEEE, Mohammad Amir Fallah, Mehdi Rasti, *Senior Member*, IEEE, Matti Latva-Aho, *Senior Member*, IEEE, and Merouane Debbah, *Fellow*, IEEE

***Abstract*— Spot beamfocusing (SBF) is the process of focusing the signal power in a small spot-like region in the 3D space, which can be either hard-tuned (HT) using traditional tools like lenses and mirrors or electronically reconfigured (ER) using modern large-scale intelligent surface phased arrays. ER-SBF can be a key enabling technology (KET) for the next-generation 6G wireless networks offering benefits to many future wireless application areas such as wireless communication and security, mid-range wireless chargers, medical and health, physics, etc. Although near-field HT-SBF and ER-beamfocusing have been studied in the literature and applied in the industry, there is no comprehensive study of different aspects of ER-SBF and its future applications, especially for nonoptical (mmWave, sub-THz, and THz) electromagnetic waves in the next generation wireless technology, which is the aim of this paper. The theoretical concepts behind ER-SBF, different antenna technologies for implementing ER-SBF, employing machine learning (ML)-based schemes for enabling channel-state-information (CSI)-independent ER-SBF, and different practical application areas that can benefit from ER-SBF will be explored.**

***Index Terms*— Spot beamfocusing (SBF), near-field, electronically reconfigurable, machine learning, Fresnel region, wireless**

I. Introduction

The terms beamforming and beamfocusing have different interpretations in the literature. Therefore, first, we clarify the definitions of these terms as they are used in this article. **Beamforming** is a technique that directs a wireless signal towards a specific receiving device, rather than spreading the signal omnidirectionally. **Beamfocusing** is a special kind of 3D-beamforming where most of the radiated power is concentrated in a confined focal region around a point in the 3D space, defined by both angular (azimuth and elevation angles) and radial domains. This is unlike traditional 2D beamforming, which only considers the angular domain. We use the term spot beamfocusing (**SBF**) for the special case where the focal region of beamfocusing is very small, i.e., the power is focused in a spot-like region around the focal point [1]. In this paper, we study the SBF for electromagnetic signals. SBF has many potential applications not only in wireless communication and wireless power transfer (WPT) but also in health and medical sensing (e.g., stimulating specific neurons through neuromodulation [2]), semiconductor and THz technology (e.g., high speed turning on/off nano switch arrays through casting spot-like power on each switch element [3]), the study of matters through THz spectroscopy [4], etc.

The implementation of the SBF in these various applications is generally realized hard-tuned (HT), or electronically reconfigured (ER). In hard-tuned SBF (**HT-SBF**), there exists no soft control on the location of the focal point, while electronically reconfigurable SBF (**ER-SBF**) schemes can adjust the focal point by softly configuring the radiated beam of the aperture. In general, due to the limitations of HT-SBF, ER-SBF schemes are preferred which are elaborated in what follows.

HT-SBF is generally implemented through lenses, mirrors, or gratings [5]. *Lenses* are devices that refract or bend the beam passing through them according to their shape and material, as well as the wavelength of the signal. Lenses are either convex or concave; convex ones can focus the beam to a region or a point. *Mirrors* are like lenses, however, instead of passing the beam through, they reflect the beam; and if properly designed, all reflected signals can be added constructively in the focal point, leading to the SBF. A *Grating* is a component that contains a microscopic and periodic groove structure, which splits incident electromagnetic waves into multiple beam paths through diffraction. This causes signals of different wavelengths to propagate in different directions. By carefully designing the groove structure of the grating, it is possible to concentrate the beam in a desired region/point.

Traditional HT-SBF technologies face challenges such as diffraction, and aberrations, alignment mismatch [6], as well as fixed focal points. There exist limited mechanical methods to change the desired focal point (DFP) location, such as employing stepper motors. However, they are rather slow and non-flexible, have limited control over the DFP position, and require regular maintenance services. On the other hand, HT-SBF systems struggle with wavelength-dependent focal points and environmental changes affecting signal propagation, resulting in the potential deviation of the achieved focal point (AFP) from the DFP. Considering these limitations, a more flexible and potentially cheaper option is to implement ER-SBF through intelligent apertures. ER-SBF requires extremely large-scale apertures [7] and can be realized through different antenna technologies such as conventional phased array antennas (CPAs) [8], dynamic metasurface antennas (DMAs) [9], and holographic MIMO (HMIMO) surfaces [10]. While HT-SBF and ER-beamfocusing have been widely studied in the literature so far and implemented in many optical and non-optical electromagnetic applications, there exists no comprehensive study of different aspects of smart ER-SBF systems and their future applications, especially for nonoptical (mmWave, sub-THz, and THz) electromagnetic waves in the next generation wireless technology.

In this regard, we are going to address the following key questions:

- Given that the near-field propagation region allows for 3D beamfocusing, can this technique be applied to the far-field region too? If yes, what are the key enabling technologies (KETs) that facilitate this process?
- How can near-field ER-beamfocusing be extended to near-field ER-SBF?
- What are the challenges, advantages, and disadvantages associated with deploying ER-SBF using various smart antenna technologies? Additionally, how do design parameters (such as frequency, spacing between array elements, antenna size, and channel estimation accuracy) impact the performance of ER-SBF?
- How can machine learning techniques be leveraged to enhance the performance of ER-SBF systems?
- What are the potential applications of ER-SBF in different domains?

In the following sections, we address these research questions.

II. Beamfocusing in different propagation zones

A. *Is 3D beamfocusing possible in far-field?*

To begin with, we explore the case of signal propagation and beamforming in the far-field region. This is defined as the region where the distance from the measuring point to the transmitting aperture exceeds the Fraunhofer limit D^F. The Fraunhofer limit can be approximated by $D^F \approx 2D^2/\lambda$ [11] where D is the diameter of the aperture and λ is the wavelength. To have some idea about the approximate far-field region for phased-array antennas operating in RF, mmWave, sub-THz, and THz frequencies, consider a 60×60 phased-array antenna wherein the distance between neighboring array elements is Δd. For sample frequencies of 3GHz, 30GHz, 300GHz, and 3THz, and assuming $\Delta d = 0.5\lambda$, the Fraunhofer limit corresponds to 360m, 36m, 3.6m, and 36cm respectively.

The realization of sharp and even pencil beamforming is achievable through far-field beamshaping schemes in the *angular domain*, but the implementation of *3D beamfocusing* requires the *radial domain* beamfocusing as well, which is not feasible through a *single* transmitting aperture due to the monotonically decreasing power level in the radial domain in the far-field region. This is shown in Fig. 1-a, where a single phased-array (PA) aperture located on xz-plane is designed to transmit a sharp beam toward the UE located at some point in the far-field region. It is seen that the implementation of angular directivity is available here, however, it is not possible to focus the beam at any point in the y direction (corresponding to r in the spherical system in this case).

Although 3D far-field beamfocusing is not feasible through a single aperture, it can be enabled by some technologies that implement beamforming through a set of synchronized geographically distributed access points (APs). Cell-free massive MIMO is one such technology that is regarded as one of the components of the upcoming sixth-generation (6G) networks. Besides the basic advantages including the improvement of the coverage and capacity compared to traditional cellular networks, cell-free massive MIMO can also be considered as a key enabling technology (KET) for providing 3D beamfocusing in the far-field region. In this regard, consider that some UE is served by a set of APs in a cell-free network as seen in Fig. 1-b, and each serving AP is equipped with a large-scale phased-array antenna through which a directional beam is radiated toward the UE. The signal from one AP can interfere with the signals from other APs at the UE location, but this interference can be constructive if they have minimal phase mismatch. This requires exact synchronization of all APs, which is expected for the next generation of cell-free wireless networks. This way, beamfocusing is achieved because a local maximum power can be measured at the desired location due to the synchronized arrival of beams at the DFP, while the power decays around that point due to phase mismatch of the arrived beams there. The feasibility of achieving a sharp beamfocusing for each UE depends on several factors, such as the availability of a sufficient and evenly distributed number of serving APs around the UE, the accurate synchronization of the serving APs, and the large antenna array size for each AP, which enables narrow-beam transmissions toward the UE. A similar setup for far-field beamfocusing can be implemented using a set of fully synchronized reconfigurable intelligent surfaces (RISs) around the UE, as shown in Fig. 1-b.

B. *Near-field (Fresnel) beamfocusing*

Unlike the far-field scenario, where 3D beamfocusing is impossible with a single aperture, in the near-field we may focus the radiated signal power around a desired point through a single PA. However, beamfocusing is not feasible in the non-radiative near-field region, where the DFP is very close to the radiating aperture. This is because this region is dominated by the static inductive/capacitive fields, not by electromagnetic radiation. Near-field beamfocusing is feasible in the *radiative near-field* region wherein the distance from the aperture (r) lies in the region $D^N < r < D^F$ where D^N is a small distance very close to the antenna (usually lower than a wavelength) beyond which the radiative active power dominates the non-radiative reactive power.

In the far-field region, all elements of the radiating aperture can be viewed as a single point source, and therefore, a change in r leads to an equal change in the arrival phase of signals from all array elements, resulting in no directivity change relative to the isotropic antenna in this direction. However, this does not hold in the near-field scenario due to the spherical wave-front in the near-field region. More specifically, by applying appropriate phase shifts to each antenna element of the PA, we can set the received signals radiated from each antenna element to be constructively (i.e., coherently) added at the DFP; however, since different channel phase shifts are experienced for each antenna element at points around the DFP, power decay might be experienced at these points, leading to 3D beamfocusing at the DFP. This is illustrated in Fig. 2-a.

III. Near-field (Fresnel) ER-SBF

A. *From beamfocusing to ER-SBF*

Consider a single phased-array aperture. For a given beamforming vector $\boldsymbol{w}$, let define the beamfocusing radius (**BFR**)

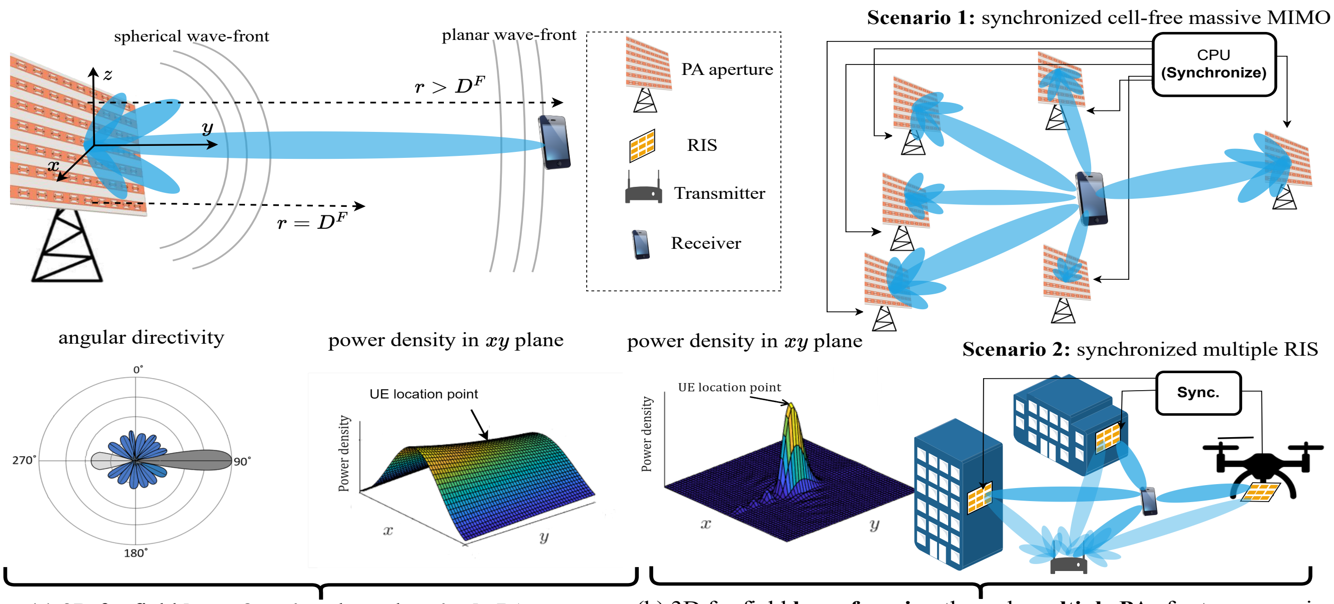

(a) 2D far-field **beamforming** through a **single PA** aperture (b) 3D far-field **beamfocusing** through **multiple PAs** for two scenarios

Fig. 1: (a): A single phased-array aperture with 2D beamforming toward the UE in the far-field region. Beamforming is possible in the angular domain, but not in the radial domain in the y-axis direction. (b): Two scenarios for the implementation of far-field 3D beamfocusing through transmissions of a set of distributed fully synchronized apertures, including a cell-free network, and a network of synchronized RISs.

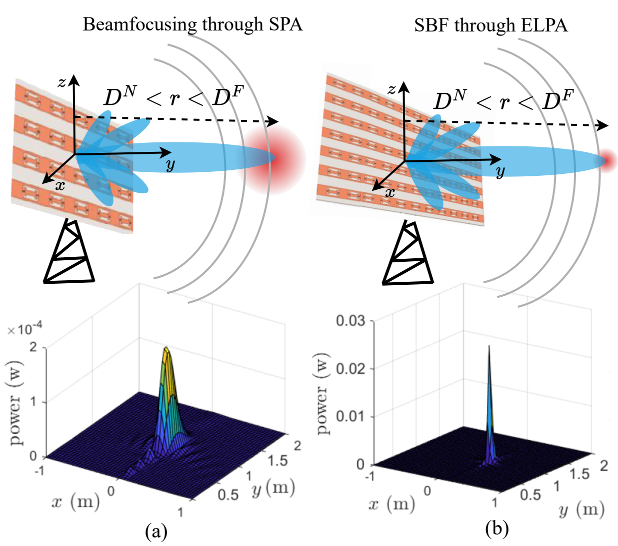

Fig. 2: Near-field beamfocusing showing spacial power density on the xy plane for an aperture located on xz plane for DFP at (0,1,0). The antenna elements are half wavelength apart and the frequency is 28GHz. The left figure shows the beamfocusing for a 6×6 SPA and the right one shows the SBF through a 60×60 ELPA.

denoted by R at some reference plane S, as the radius of the circle S_R located on the reference plane and centered at DFP which contains a fraction η of the total radiating power in the reference plane S [1]. For example, a BFR value corresponding to $\eta = 0.9$ implies that a circle of radius BFR centered at DFP contains 90% of the total radiating power at the reference plane. Considering a sphere of radius R at the DFP, it can be shown that when the near-field impact becomes dominant, the power level fades outside the sphere in all directions, even when getting close to the aperture [1]. This implies that the focal region in the near-field can be imagined as a sphere centered at the DFP. We are specifically interested in obtaining an electronically controlled spot-like beamfocusing (i.e., ER-SBF) with a high power density and minimal BFR (close to zero) at the DFP. This is the key point in utilizing this technology in many practical applications, overtaking the benefits of many traditional beam spotting technologies such as lenses, mirrors, and gratings. In practice, higher frequencies can realize sharper SBFs.

To achieve near-field SBF, a high value of the ratio D/λ is required [7], which can be accomplished through decreasing λ as well as increasing D. The former is achieved through transitioning to mm-wave/THz frequencies. The latter can be realized by using extremely large-scale phased-arrays (ELPAs) rather than small-scale phased-arrays (SPAs). For instance, the spatial power distribution in the xy plane around the DFP at (0,1,0) for an aperture located at xz plane and centered at the origin is illustrated in Fig. 2 for two scenarios: a 6×6 SPA and a 60×60 ELPA operating at 28 GHz. The figure demonstrates that the SPA enables beamfocusing, however, the SBF can only be achieved by the ELPA, which attains a much higher power intensity and a much lower BFR at the focal point, as well as much smaller side lobes elsewhere. The SBF problem for a phased-array antenna requires finding the beamforming coefficients corresponding to minimum BFR at the DFP; this problem is generally non-convex, NP-hard, and intractable; however for ELPAs in the Fresnel region, which is the case for realizing ER-SBF, the problem is equivalent to finding the solution to the problem of maximizing the received power at the DFP, which is tractable and less complex than the original problem ([1]). It should be noted that the realization of a sharp focal point requires that $r \ll D^F$ [12]. This means that SBF is not feasible at regions close to the boundary of far-field and near-field.

Various aspects of the implementation of ER-SBF can be explored. In what follows we elaborate on one aspect. Let Δd be the distance between adjacent elements of the ELPA. If we consider a given number of array elements for the ELPA, a key question is how to determine the optimal value of $\Delta d/\lambda$ for achieving the best SBF. In practice, this ratio is usually selected as 0.5 for non-holographic CPA/DMA apertures in applications involving far-field/near-field beamforming. However, the SBF performance is sensitive to the ratio $\Delta d/\lambda$, which affects it differently than regular beamforming applications. Considering $\Delta d/\lambda \in \{0.5, 1, 1.5\}$ as an example, Fig. 3-a illustrates the normalized absolute value of the power density in the y direction for a 60×60 ELPA located on the xz plane centered at the origin, operating at frequency 28GHz, and whose DFP is at (0,1,-0.5) which is 1.12m away from the center of the aperture. It is seen that the maximum peak power received at the DFP occurs when $\Delta d/\lambda = 0.5$. This is because increasing $\Delta d/\lambda$ makes some array elements farther from the DFP, which reduces channel gains and the aggregate peak power. However, higher values of $\Delta d/\lambda$ result in lower BFR. Here, instead of the BFR, we have specified the more simplistic case of half-power beam width (HPBW). For example, for a fixed value of λ, increasing $\Delta d/\lambda$ increases the aperture diameter, which enables higher near-field benefits of achieving sharper beam focus and lower BFR. Therefore, a tradeoff between high received power and low BFR should be considered. For instance, changing $\Delta d/\lambda$ from 0.5 to 1 decreases the measured power density at DFP by only 4%, while the HPBW is highly improved from 8.5cm to 4.9cm. A higher aperture diameter can also be achieved by using a higher number of array elements instead of increasing $\Delta d/\lambda$. However, this requires more expensive hardware and complex beam-tuning software, which might not always be preferred. It should be noted that increasing $\Delta d/\lambda$ from 0.5 has the benefit of creating a sharply focused beam with fewer antenna elements, however, this makes the antenna sparse, which in turn, may lead to the occurrence of additional focal points due to near-field grating lobes. Another technical aspect of ER-SBF is the elaboration of cost per BFR. Fig. 3-c depicts the performance of SBF in terms of HPBW versus the number of antenna rows/cols for the simulation scenario same as that in Fig. 3-b, but with $\Delta d = 0.5\lambda$, and considering a various number of antenna elements. Assuming that the complexity and cost of the SBF structure are proportional to the number of antenna elements, the figure shows how increasing the cost leads to a smaller focal region.

B. *Different technologies for realizing ER-SBF*

In what follows, we briefly introduce various antenna technologies for the implementation of ER-SBF.

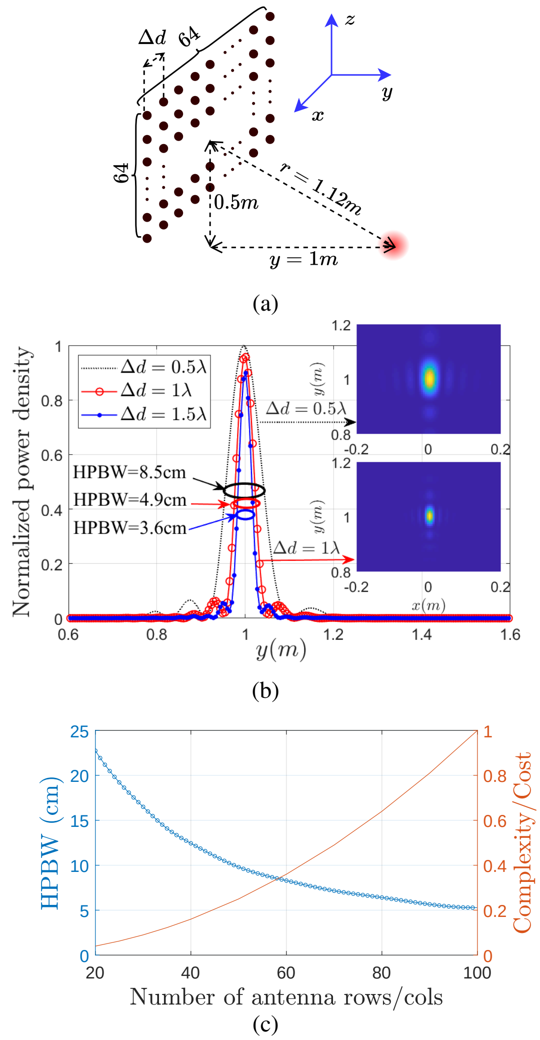

Fig. 3: (a): 60×60 ELPA for realizing ER-SBF. (b): Power density versus distance (y) for $\Delta d/\lambda \in \{0.5, 1, 1.5\}$. (c): Complexity/cost, as well as HPBW versus number of antenna rows/cols for $\Delta d = 0.5\lambda$.

CPAs: Conventional phased-array antennas can utilize active or passive elements for adjusting amplitude/phase to implement the SBF at given DFP locations; CPAs are typically suitable for SBF through large apertures at RF frequencies. At RF bands, large CPAs employing high-power transmitters can generate a focal point at distances ranging from tens to hundreds of meters, potentially with higher focused power levels at the DFP compared to other technologies.

DMAs: Metamaterials indicate a class of artificial composite materials capable of interacting with incident electromagnetic waves, showing a path to highly low-cost, mass-producible reconfigurable apertures that can be manufactured in dense and large-scale ultra-thin microstrip structure [9]. DMAs employ arrays of programmable meta-atoms that can be manufactured in various sizes, enabling ER-SBF for a variety of applications in mmWave, sub-THz, and THz frequency bands. To achieve perfect SBF at the precise location of DFP with minimal BFR, each element of the metamaterial ELPA should be provided with analog full-scale phase control or discretized control with low quantization error.

HMIMO surfaces: HMIMO surfaces provide 3D beamshaping with the help of holographic surface (HS) and electromagnetic signal technology [10]. HMIMO surfaces consist of large and dense elements (with spacing between antenna elements usually much smaller than half a wavelength) and can be manufactured with or without metamaterials. HMIMO antennas manipulate beamshaping through kinds of holographic patterns on the aperture surface. They can dynamically control the phase/amplitude of array elements if they are reconfigurable. Reconfigurable holographic surfaces (RHSs) employ tunable elements to adjust the phase/amplitude at different parts of the radiating aperture. For static holographic surfaces (SHSs) however, the control on phase/amplitude is more limited and the directivity is mostly determined by a predesigned hologram pattern. A holographic pattern can somehow be calculated/recorded at the design time and applied on the aperture surface. Considering the hologram pattern, by applying specific electromagnetic signals through one or multiple feeds (where the number of feeds is much less than the number of radiating elements), a beam with a desired directivity pattern is transmitted. An SBF can be formed at a given DFP by designing the hologram pattern carefully. HMIMO surfaces use different structures than other phased-array antennas to implement amplitude/phase tuning, including holographic-based leaky-wave antennas (LWAs) and photonic tightly coupled antenna arrays (TCAs) [10]. This results in replacing a large amount of costly and power-hungry RF devices, leading to much cheaper solutions. Although HMIMO surfaces can focus the beam very exactly at the DFP location, due to the limited number of feeds, and limited mechanisms for changing the directivity, a less flexible soft-tuning DFP is available here compared to other technologies.

In summary, CPAs and DMAs utilize the idea of constructive interference of array elements at the DFP to form SBF. HMIMO surfaces however reconstruct the desired SBF through diffraction of the electromagnetic wave according to a hologram. The diffracting radiation of HMIMO surfaces prevents the realization of high-power SBF at the DFP. CPAs are preferred when the target point is subject to high dynamics, or high-power SBF at longer distances is required. Conversely, if high static resolution, as well as low cost and compactness of the antenna structure, are taken into account, holographic surfaces provide a superior solution. DMAs, on the other hand, combine the benefits of both CPAs and HMIMO surfaces.

C. CSI estimation for ER-SBF

ER-SBF requires the exact CSI of all array elements of ELPA. This can be achieved in one of two ways: (a) similar to the assumption made in HT-SBF systems, if the exact location of the DFP, as well as the exact channel model, are known, exact CSI is obtained according to the model, or (b) by employing near-field CSI estimation techniques. Existing channel estimation methods for ELPA and massive MIMO antennas rely heavily on channel sparsity in the angular domain, which is only valid for planar wavefront assumptions in far-field propagation. Recently, the authors of [13] proposed a polar-domain sparse representation of the channels with a compressive ratio of about 50% for a 256-element antenna. However, this idea only works for 1D linear arrays and does not apply to the 2D ELPAs employed for ER-SBF.

In the near-field, the channel coefficients matrix is not sparse due to the spherical wavefront, even for the simple case where no multi-path propagation exists. Considering this, together with the extremely large number of antenna elements required for ER-SBF, the conventional channel estimation methods employed for massive MIMO are impractical to near-field ELPAs due to very high pilot overhead and processing overload. Two ML-based schemes might be applied to overcome this problem: (a) applying ML to estimate CSI [14], or (b) applying CSI-independent ML algorithms to adaptively focus the beam at the DFP [1]. This is further elaborated in the following subsection.

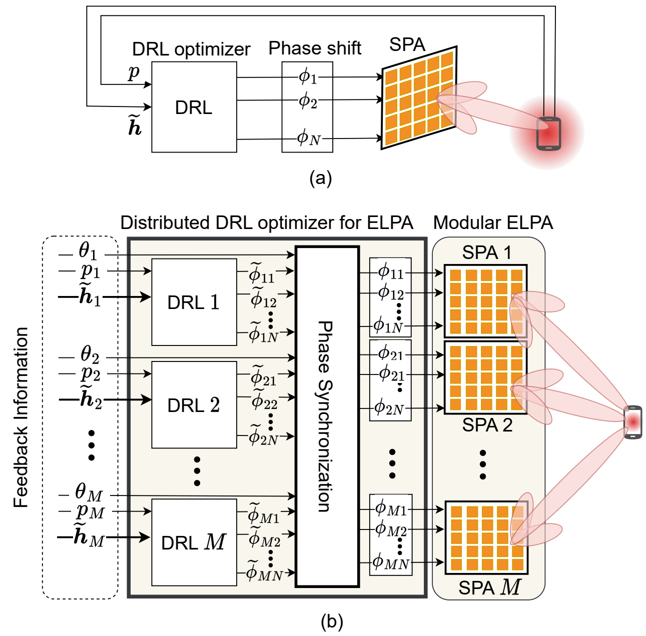

Fig. 4: Implementation of ML-based ER-SBF. (a): DRL-based beamfocusing for a SPA. (b): distributed DRL-based SBF through an ELPA consisting of a set of SPAs.

D. Application of Machine Learning and Transfer Learning for ER-SBF

ML can enhance the performance of ER-SBF systems, enabling adaptive and precise SBF for cases where the CSI is unknown or inexact. Fig. 4-a shows a proposed ML structure for near-field beamfocusing through a deep reinforcement learning (DRL) optimizer for an N-element SPA. The DRL block receives the CSI estimation (if available), as well as the power level measured by the UE at each learning epoch, and then it calculates the next step beamforming vector $\boldsymbol{\phi} = [\phi_1, \phi_2, ..., \phi_N]$. The procedure continues until the output response converges and the DRL learns the optimal vector $\boldsymbol{\phi}^* = [\phi_1^*, \phi_2^*, ..., \phi_N^*]$ that corresponds to the maximum focused power.

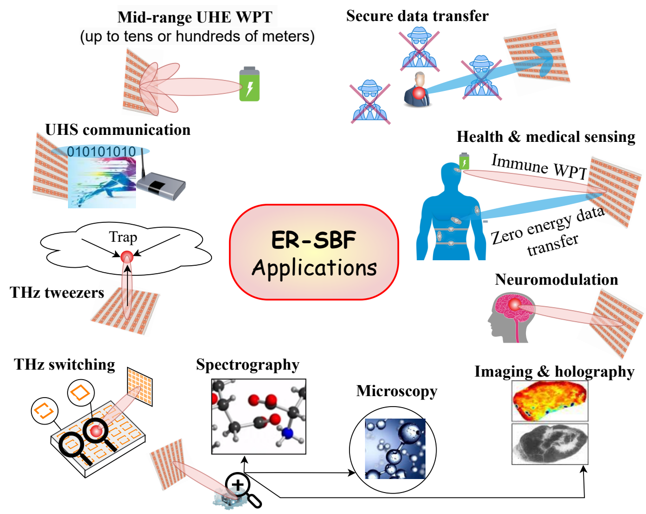

Fig. 5: The schematic diagram of several practical applications of the Fresnel ER-SBF is presented.

The proposed structure of Fig. 4-a only works for beamfocusing using SPAs. However, SBF requires ELPAs with extremely large action space, where conventional ML schemes cannot handle the computational complexity in the original form. For example, a 60×60 ELPA with 4-bit phase shifters has an action space with a cardinality of 16^{3600}, which is too large and unaffordable for a single DRL. A good idea is to split the ELPA into a set of SPAs each equipped with a DRL optimizer to collaboratively (i.e., synchronously) focus the beams and form the overall spot-like highly concentrated power at the DFP [1]. For example, a 3600-element ELPA can be split into 100 SPAs each having 6×6 antenna elements. The schematic of the proposed structure is depicted in Fig. 4-b, wherein a $M \times N$ element ELPA is split into M sub-arrays each having N antenna elements. It is seen here that for each sub-array m, in addition to the measured power p_m and (possibly) estimated CSI vector $\widetilde{\boldsymbol{h}}_m$, the arrival phase θ_m is also required by the DRL to align all elements $\widetilde{\phi}_{mn}$ through the phase synchronization block. This block subtracts the offset θ_m from all elements of $\widetilde{\phi}_{mn}$ and obtains the new beamforming elements ϕ_{mn} so that all radiated beams are added coherently and constructively at the UE location, leading to the desired SBF directivity pattern.

In practice, all SPAs have identical structures. Noting the domain alignment of the sub-arrays, having single or multiple trained *teacher* SPAs, the remaining SPAs do not require learning from scratch, rather, different schemes of *transfer learning* can be applied to speed up the learning process of remaining *student* SPAs. A similar idea can be employed for learning the whole ELPA for a new DFP when it has been previously trained for some other nearby DFPs. This can effectively handle the mobility management of the UE.

IV. Application Areas of ER-SBF through ELPAs

There exists a variety of applications in physics, wireless communication, WPT, medical and health, etc., which can be highly benefited from ER-SBF, some of which are schematically presented in Fig. 5. In what follows we briefly introduce some of these applications.

Ultra-high-speed (UHS) wireless communication: ER-SBF can provide the UE with UHS data transfer, much faster than achieved through conventional beamforming/beamfocusing schemes. The reason behind that is manifold. From the UE side, casting of all transmitted power to the exact UE location point results in ultra-high SNR leading to ultra-high Shannon's channel capacity. From the network side, almost the whole spectrum (with minimal interference) can be shared among different users in different spots in the network, leading to full-scale 3D spatial spectrum reuse and very high aggregate throughput of the UEs in the network. In addition, by employing HMIMO communication, a higher number of spatial degrees of freedom (DoF) can be achieved leading to the achievement of higher data rates [10].

Mid-range safe and ultra-high-efficiency (UHE) WPT: Mid-range WPT for wireless battery charging and energy transfer through ER-SBF will potentially be a key enabling technology (KET) in the next generation of wireless networks. Nowadays, the industry offers low-range WPT battery charging facilities that require the UE to be in the non-radiative near-field region, very close to the power transmitting antenna. Health hazards are the main barrier to extending the wireless battery charging distance from low-range distances (in the order of several centimeters) to mid-range distances (in the order of several meters). In the far-field beamforming, there exists a health hazard if some body tissues are placed between the radiating antenna and UE. By using Fresnel ER-SBF, we can precisely cast almost all signal power to the exact energy harvesting antenna with negligible unwanted energy attraction in any other points in the 3D surrounding space, leading to optimal and safe WPT.

Secure data transfer: ER-SBF can greatly improve the security level of data transfer. In particular, dense IoT devices with limited resources might be easily exposed to eavesdropping by unauthorized receivers. By focusing all transmitted data energy exclusively on the intended receiver, ER-SBF effectively places all eavesdroppers within the blind zone. Consequently, ER-SBF thwarts eavesdroppers' ability to intercept the data at the physical layer, even if they are situated between the transmitter and the intended receiver.

Health and medical sensing: There exists a variety of tiny health sensors and electronic chips that might be implanted inside the body of a patient and remain there for several years, or even throughout the lifetime. Safe battery charging is a necessity here which might be achieved through WPT with some external radiating antenna. Precise spot beamfocusing is essential here because a slight absorption of radiated power by some tissues near the sensing device can be very harmful and cause serious health risks. On the other hand, due to limited battery capacity, a zero-energy data transfer strategy is essential for sending sensed data from inside the body to a data collector outside. Here again, to achieve an acceptable SNR, SBF data transfer requires minimal transmitted power compared to any other beamforming technique, leading to minimal battery consumption.

Neuromodulation: Neuromodulation is a technology that impacts the activity of nerves through targeted delivery of a stimulus to the intended nerves or specific neurological sites in the body [2]. Neuromodulation usually involves delivering electrical or pharmaceutical agents directly to a target area; however, recently the electromagnetic stimulus has become more popular because of the much more flexibility, ease of implementation, and soft control on the targeted beam [15]. ER-SBF operating at sub-THz and THz frequencies, enables precise soft control of the electromagnetic beam, allowing for targeted stimulation of nerves at specific intended locations.

THz switching: THz switching refers to the ability to turn on/off a specific switch (from an array of switches) on a time scale of picoseconds through casting THz electromagnetic stimulus on the intended switch. ER-SBF in sub-THz and THz frequencies can be used to fast and softly steer and focus the stimulating power on any desired switch [3].

Other applications that may benefit from ER-SBF include THz tweezers, microscopy, spectrography, etc., which are not investigated here.

References

[1] M. Monemi, M. A. Fallah, M. Rasti, and M. Latva-Aho, "6G Fresnel Spot Beamfocusing using Large-Scale Metasurfaces: A Distributed DRL-Based Approach," *submitted to IEEE Transactions On Mobile Computing*, vol. 1, no. 1, p. 1, 2023, preprint available at http://arxiv.org/abs/2311.11109.

[2] E. Krames, P. H. Peckham, and A. R. Rezai, *Neuromodulation: comprehensive textbook of principles, technologies, and therapies*. Academic Press, 2018.

[3] H. Ou, F. Lu, Y. Liao, F. Zhu, and Y.-S. Lin, "Tunable terahertz metamaterial for high-efficiency switch application," *Results in Physics*, vol. 16, p. 102897, 2020.

[4] J. Neu and C. A. Schmuttenmaer, "Tutorial: An introduction to terahertz time domain spectroscopy (THz-TDS)," *Journal of Applied Physics*, vol. 124, no. 23, 2018.

[5] L. C. Botten, M. Cadilhac, G. Derrick, D. Maystre, R. McPhedran, M. Nevière, and P. Vincent, *Electromagnetic theory of gratings*. Springer Science & Business Media, 2013, vol. 22.

[6] A. R. Bayanna, R. E. Louis, S. Chatterjee, S. K. Mathew, and P. Venkatakrishnan, "Membrane-based deformable mirror: intrinsic aberrations and alignment issues," *Applied Optics*, vol. 54, no. 7, pp. 1727–1736, 2015.

[7] J. Goodman, "Introduction to Fourier Optics, (WH Freeman Press)," 2017.

[8] A. Kharalkar, A. Batabyal, R. Zele, and S. Gupta, "A Review of Phased-Array Receiver Architectures for 5G Communications," in *2022 IEEE Region 10 Symposium (TENSYMP)*. IEEE, 2022, pp. 1–6.

[9] S. Kumar and H. Singh, "A comprehensive review of metamaterials/metasurface-based MIMO antenna array for 5G millimeter-wave applications," *Journal of Superconductivity and Novel Magnetism*, vol. 35, no. 11, pp. 3025–3049, 2022.

[10] T. Gong, P. Gavriilidis, R. Ji, C. Huang, G. C. Alexandropoulos, L. Wei, Z. Zhang, M. Debbah, H. V. Poor, and C. Yuen, "Holographic mimo communications: Theoretical foundations, enabling technologies, and future directions," *IEEE Communications Surveys & Tutorials*, pp. 1–1, 2023.

[11] K. T. Selvan and R. Janaswamy, "Fraunhofer and Fresnel Distances: Unified derivation for aperture antennas." *IEEE Antennas and Propagation Magazine*, vol. 59, no. 4, pp. 12–15, 2017.

[12] D. R. Smith, V. R. Gowda, O. Yurduseven, S. Larouche, G. Lipworth, Y. Urzhumov, and M. S. Reynolds, "An analysis of beamed wireless power transfer in the fresnel zone using a dynamic, metasurface aperture," *Journal of Applied Physics*, vol. 121, no. 1, 2017.

[13] M. Cui and L. Dai, "Channel estimation for extremely large-scale MIMO: Far-field or near-field?" *IEEE Transactions on Communications*, vol. 70, no. 4, pp. 2663–2677, 2022.

[14] X. Zhang, Z. Wang, H. Zhang, and L. Yang, "Near-field channel estimation for extremely large-scale array communications: A model-based deep learning approach," *IEEE Communications Letters*, 2023.

[15] M. S. George, "Current state of electromagnetic neuromodulation therapy," *Brain Stimulation: Basic, Translational, and Clinical Research in Neuromodulation*, vol. 14, no. 6, p. 1735, 2021.